

## DESIGN AND ANALYSIS METHODS FOR UAV ROTOR BLADES

Alexandru DUMITRACHE\*, Mihai-Victor PRICOP\*\*, Mihai-Leonida NICULESCU\*\*, Marius-Gabriel COJOCARU\*\*, Tudor IONESCU\*\*\*

\*Institute of Mathematical Statistics and Applied Mathematics, Bucharest, Romania  
(alexandru.dumitrache@ima.ro)

\*\*National Institute for Aerospace Research “Elie Carafoli”, Bucharest,  
Romania (pricop.victor@incas.ro, niculescu.mihai@incas.ro,  
cojocaru.gabriel@incas.ro)

\*\*\*Politehnica University of Bucharest, Romania (tudor.ionescu@acse.pub.ro)

DOI: 10.19062/2247-3173.2017.19.1.48

**Abstract:** A design method and analysis tool of an UAV propeller based on Blade Element Momentum Theory (BEMT) for low-Reynolds number flow is presented. BEMT is completed with 3D equilibrium- implementation, a post-stall model and swirl velocity considerations to improve the accuracy of the results. An open-source code, JBlade, based on BEMT is used to obtain performance curves in off-design cases for a given propeller. Finally, the results are analyzed for a UAV Hirrus propeller. This methodology can be used successfully in the preliminary design phase of an UAV propeller, whose data can then be used as input in an optimization method.

**Keywords:** combustion chamber, CFD, methane combustion, turbulent flow

### 1. INTRODUCTION

The propeller has several application areas, but the most spectacular application is its use as a propeller propulsion system, particularly for aircraft. It has been found that the use of propeller engines driving becoming more improved is not enough without the improved propeller efficiency, requiring theoretical and experimental studies [1], [2].

The procedure used in aerodynamic design of a propeller is essential to determine aerodynamic loads on the basis of which the required thrust and torque are then determined. The most important aerodynamic characteristics of the propeller, the efficiency and the power required are then obtained from the values of thrust and torque. Since these loads must be accurately determined for different operating conditions of the propeller, the choice of the calculation method is an important issue.



FIG. 1. Small UAV launch from an air-powered catapult.

In recent years more researches on unmanned aircraft (UAV) have been carried out, especially for those of small size, since they are less observable and they can be exploring in smaller spaces. In these conditions the study of suitable profiles of rotor blades used in propelling of these aircrafts. i.e. at low Reynolds numbers, has been imposed. Although UAV systems are composed of several elements apart from air vehicle, they are usually classified based on the capacity of air vehicle to perform the required tasks [3].

The development of advanced small or micro- UAVs is hampered by a number of technology gaps including: insufficient analysis methods for low Reynolds number aerodynamics, combined battery-motor-propeller propulsion, control effectiveness estimation, and weight estimation.

It is known that the main task during the introduction stage of aeroplane design is to determine the basic aeroplane performance. The thrust curve of the power plant is one of the input data, i.e., available thrust versus flight velocity. That means it is necessary to obtain this characteristics curve for a propelled aeroplane.

## **2. OVERVIEW ON THE AERODYNAMIC CALCULUS OF A PROPULSIVE PROPELLER**

Depending on the design stage of the airplane (preliminary or final), the aerodynamic calculus of a propeller can be carried out using empirical methods, theoretical methods or a combination of those (the hybrid method).

Since the propeller plane is powered by a reference propeller, the propeller plane theory has been chosen as the basis of the theory propeller for UAVs. The speed of movement mentioned above must be sufficient to provide a lifting force on the UAV's wing, which is equal to the weight of the plane. The propulsion propeller can be defined as consisting of a number of blades which are identical and arranged radially, and equiangular, forming the rotor. By means of an engine, these blades are rotated around the axis of the impeller.

The thrust required to move an UAV is produced by one or more UAV propellers.

It is considered that any blade cross-section has the shape of an airfoil. By his movement through the fluid, on any element of the blade, the drag and lift forces are exerted.

The blade, like the profiles, executes a rotating motion with angular velocity  $\Omega$  and a translatory speed  $V_\infty$ , the resultant motion velocity is the velocity  $W$  of the profile considered at rest air from the upstream infinity.

The design of an airplane propeller and a given engine has three phases:

1) the establishment of the basic kinematic parameters of the propeller (usually as basic kinematic parameters the flight speed and rotational speed of the propeller are selected);

2) the establishment of the basic geometric parameters of the propeller (as the basic geometric parameters of the propeller, the diameter and the number of blades are chosen);

3) the aerodynamic calculus that includes 2 stages [1], [4]-[6]:

- determination of the propeller geometry, i.e. the variation of chord, thickness, and the twisting of the blade depending on the radius, to obtain maximum efficiency for most important operation regime of the airplane (preliminary propeller design);

- determination of the aerodynamic characteristics of the propeller.

Usually this calculation requires several iterations to obtain required performance characteristics. In general, basic kinematic parameters of the propeller are imposed by the design theme, being specific to the aircraft to be equipped with the propeller and to engine have to spin it.

Rotational speed is determined by engine power and, once chosen, determines the size of the transmission which also realizes the link between engine and propeller. By knowing the operational conditions of the propeller (the flight speed, the engine characteristic, the rotational speed of the engine and of the propeller and the maximum weight at takeoff of the plane) one can solve the indirect problem for the basic geometric characteristics of the propeller (the second stage in sequence of the aerodynamic design of the propeller plane).

The most important parameter which occurs in the design of a propeller is the diameter. The diameter of the propeller depends on several factors: the required performance of the propeller in various operating conditions, the maximum blade tip speed (which affects performance and the noise levels of the propeller), the weight of the propeller, the distance from the ground to the propeller axis.

If neglecting the influence of the induced velocity, the blade tip speed is

$$W_{\max} = \sqrt{V_{\infty}^2 + (\pi ND)^2} \quad (1)$$

or dimensionless, Mach number,  $M$ :

$$M_{\max} = M_{\infty} \sqrt{1 + (C_P/C_T)^2} \quad (2)$$

Usually, taking into account the noise level, the permissible limit is  $M_{\max} = 0.85-0.9$ . However, even in operating conditions, using the Mach number,  $M_{\max}$  can be considered acceptable at values of 250-300 m/s, however, due to high noise levels the values are limited to 250 m/s.

The influence of the diameter on the propeller efficiency is determined based on the aerodynamic characteristics of the propeller. It is necessary to choose the cruise speed of the UAV corresponding to the calculation.

The number of blades is a very important parameter in the design process of a propeller. It is chosen according to the product of the blades and propeller total activity factor. In general, activity factor (AF) for a blade has values between 80 and 180.

$$AF_{propeller} = B \cdot AF_{blade} = B \cdot (10^5/16) \int_{TD}^1 \bar{c} \cdot \bar{r}^3 d\bar{r} \quad (3)$$

These methods belong to a class of indirect solving problems to determine the geometry of the rotor, i.e. the diameter and the number of blades of the propeller

After solving the indirect problem, solving the direct problem follows, reaching the third design stage of the propeller, namely calculus of the aerodynamic characteristics of the propeller.

### Blade Element Momentum Theory (BEMT).

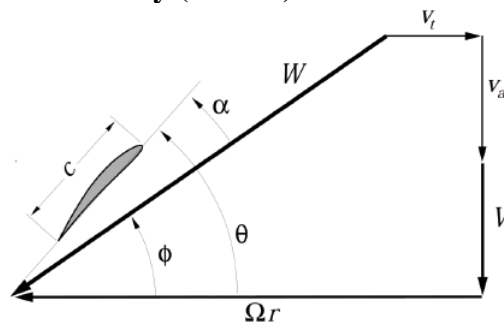


FIG. 2. Velocities at a blade element.

Combining the classical momentum theory, introduced by Froude [7] with the blade element theory enables a model of the performance of a propeller whose airfoil properties, size, and twist distribution are known. This analysis is based on the differential propeller thrust,  $dT$ , and torque,  $dQ$ , derived from momentum theory and blade element theory, being equivalent [1].

$$\left. \begin{aligned} C_a &= C_L \cos \phi - C_D \sin \phi \\ C_w &= C_L \sin \phi + C_D \cos \phi \end{aligned} \right\} F_x = \frac{1}{2} \rho W^2 c C_x \quad \left\{ \begin{aligned} T &= B \int_{R_{root}}^{R_{tip}} F_a dr \\ Q &= B \int_{R_{root}}^{R_{tip}} F_t r dr \end{aligned} \right. \quad (4)$$

To find  $\phi$  and  $W$ , the iteration variables of the classical BEM for each blade element are the axial,  $a_a$  and the tangential induction factor,  $a_t$ :

$$a_a = (W_a - V)/V \quad a_t = (W_t - \Omega r)/\Omega r \quad (5)$$

These are derived from momentum theory as:

$$a_a = \left( \frac{\sigma C_a}{4k \sin^2 \phi - \sigma C_a} \right) \quad a_t = \left( \frac{\sigma C_t}{4k \sin \phi \cos \phi + \sigma C_t} \right) \quad (6)$$

where  $\sigma$  is the local rotor solidity ratio,  $\sigma = cB/(2\pi r)$  and  $k$  is the Prandtl's correction factor that allows the blades 3D correction to the induced velocity field. The Prandtl's correction factor can be expressed simply by the following

$$k = \frac{2}{\pi} \arccos(e^{-f}). \quad (7)$$

The correction factor is used to modify the momentum segment of the BEM equations. Because for a given element, the local aerodynamics may be affected by both the tip- and hub-loss, the two correction factors are multiplied to create the total loss factor. In this case  $f$  can be expressed as:

$$f_{tip} = \frac{B}{2} \left( \frac{R-r}{r \sin \phi} \right); \quad f_{root} = \frac{B}{2} \left( \frac{r-R_{root}}{r \sin \phi} \right). \quad (8)$$

Including two-dimensional airfoil tables of lift and drag,  $C_L = C_L(\alpha, Re)$  and  $C_D = C_D(\alpha, Re)$  a set of equation is obtained that can be iteratively solved for the induced velocities and forces on each blade element.

**Low Reynolds Airfoils.** To design a propeller suitable for a UAV it is necessary, first, to know which is the size of UAV's, which is the mission to accomplished, and at what height is performed.

In the case of small UAVs, it is obvious that we are in the case of low Reynolds numbers, with some drawbacks from aerodynamics point of view. Flight at these Reynolds numbers is much less efficient than at higher Reynolds numbers and available power is a limiting technological factor at small scales. It is important to operate the airfoil at its maximum L/D operating point, but this requires operating close to the maximum steady-state lift coefficient.

We know that the most important to achieve a good performance propeller, its blade profiles must be analyzed and selected carefully.

There are now airfoils, studied (numerical or experimental) for various classes of flows at low Reynolds numbers, but not enough for small to micro UAVs.

Flow at low Reynolds numbers is dominated by viscosity, and as the Reynolds number is reduced, the effects of increasing boundary layer thickness become more pronounced.

A numerical experiment has been performed, using CFD (Fluent) [18], on a profile from known class – NACA, to obtain an airfoil polar, for a given Reynolds number (Table 1).

Leading edge separation is delayed in thin sections, with trailing edge separation delayed in thicker sections (Fig. 3). The results are higher attainable angles of attack and higher maximum steady-state lift coefficients.

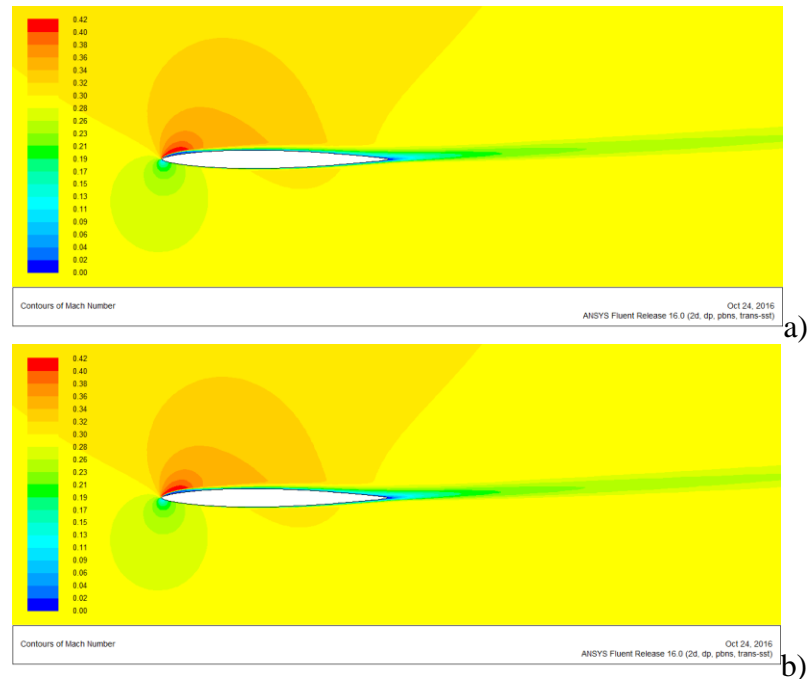


Fig. 3. Contours of Mach number for 4 deg (a) and 6 deg AOA (b) (Re = 80000)

Table 1 – Aerodynamic characteristics (Cl(alpha) and Cd(alpha)) for NACA008 (Re = 80000)

alpha (deg)	Cl	Cd
0	0	1.36E-02
2	0.1125	1.54E-02
4	0.4269	2.24E-02
6	0.55	3.80E-02

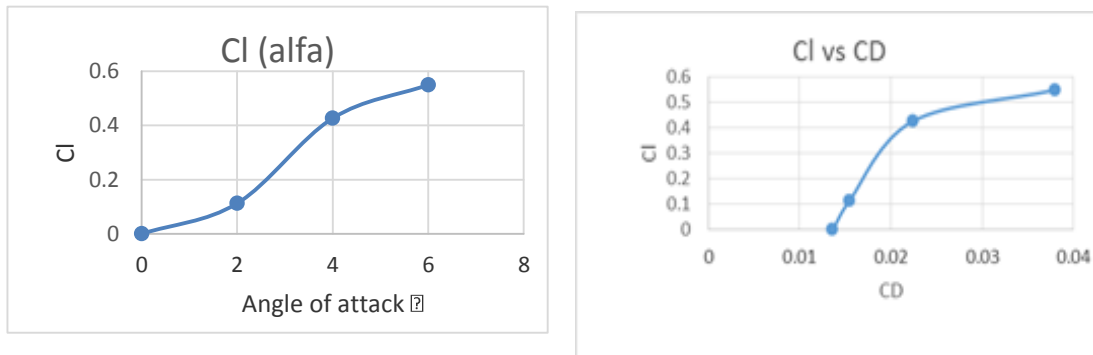


FIG. 4.  $C_L$  (alpha) and  $C_L(C_D)$  for NACA008 at Re=80000. (CFD - Ansys FLUENT)

As can be seen in Fig. 4, aerodynamic characteristics (airfoil polars) for an airfoil of a blade may be obtained using computational methods CFD (such as Ansys Fluent), but they are expensive and not justified in a preliminary design stage.

An alternative, cheaper method to obtain an airfoil polars is using the XFLR5 [16]. XFLR5 is an analysis tool for airfoils, wings and planes operating at low Reynolds numbers. It includes:

1. XFOil's Direct and Inverse Analysis capabilities.
2. Wing design and analysis capabilities based on the Lifting Line Theory, on the Vortex Lattice Method, and on a 3D Panel Method.

It is known that the Reynolds number varies along the blade and it is therefore necessary to analyze its influence on the aerodynamic characteristics for an airfoil. Using XFOIL code this influence for NACA008 is obtained, with Reynolds number varying between 60000 and 100000 (Fig. 5).

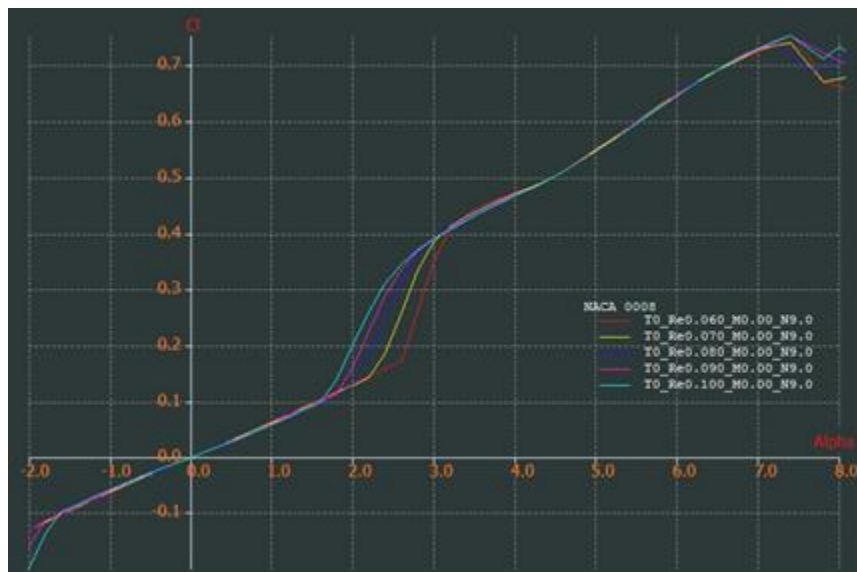


FIG. 5. Influence of Reynolds number on aerodynamic characteristics for NACA0008 ( $60000 < Re < 100000$ )

The effects of camber do not differ significantly from those at much higher Reynolds numbers, but the fact that the detailed geometry is still an effective driver of performance at such low Reynolds numbers is itself a useful conclusion (Fig. 6).

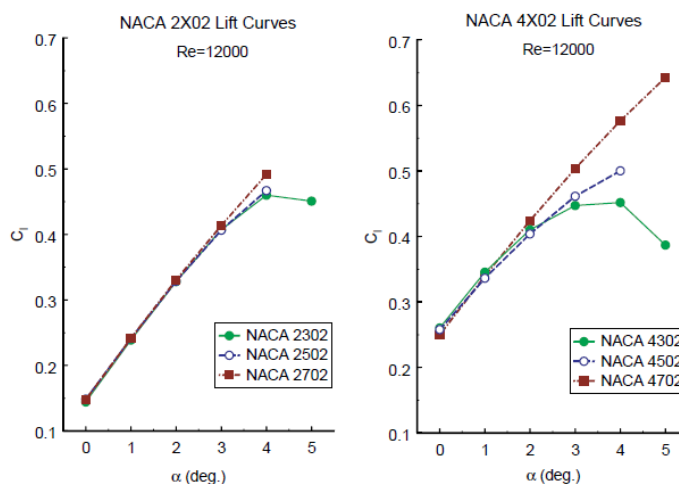


FIG. 6. Lift curves for 2% and 4% cambered NACA 4-digit airfoils at  $Re=12000$ .

It is possible to use an optimization method to obtain an airfoil with the optimum camber line and/or the thicknesses. The lack of experience at low Reynolds numbers makes optimizers an effective and important tool, not only for design, but also for enhancing our understanding of this flight regime. In the optimization design process, XFOIL can be employed for the calculation of the airfoil aerodynamic characteristics at low-speed and low Reynolds numbers, and estimate the chord-wise location of transition from laminar to turbulent flow. Thus, one can obtain an optimized version of an Eppler E387 airfoil, which already has a  $C_L/C_D$  ratio superior to other profiles, suitable for the design process of an UAV propeller blade [8].

Finally, wind-tunnel testing of low Reynolds number airfoils is, however, still needed to provide engineers with a necessary level of confidence required to make important engineering decisions.

BEMT is completed with 3D equilibrium- implementation, a post-stall model [9] and swirl velocity considerations to improve the accuracy of the results.

**Swirl Velocity Considerations.** The formulation, at this stage, incorporates only the inviscid induced tangential velocity, also referred to as inviscid swirl. In most conventional large scale, high Reynolds number applications, this is sufficient. For the small scale, very low Reynolds number applications of interest here, the viscous flow entrainment is an important consideration.

The thick wake regions generated by each blade produce a significant ‘viscous swirl’ effect. For the purpose of formulating the equations this term is incorporated by separating the tangential velocity into  $v_{\text{inviscid}}$  ( $v_i$ ) and  $v_{\text{viscous}}$  ( $v_v$ ). No viscous correction is applied to the vertical induced velocity. The viscous swirl is proportional to  $\cos(\phi)$  while any viscous downwash term would be proportional to  $\sin(\phi)$  and roughly an order of magnitude smaller than the swirl correction.

The viscous swirl is incorporated in all terms of the formulation except in the inviscid portion of the actuator ring equation for torque. The viscous losses are already accounted for in the viscous drag portion of that equation. These substitutions result in the final versions of the four basic relations:

Actuator Ring:

$$dT = 2k\rho u(u + U_\infty)(2\pi r)dr - B(C_d/C_l)(u + U_\infty)\rho\Gamma dr \quad (9)$$

$$dQ = 2k\rho v_i(u + U_\infty)(2\pi r)rdr - B(C_d/C_l)(\Omega r - v_v - v_i)\rho\Gamma rdr \quad (10)$$

where  $k$  is the Prandtl tip loss factor.

Blade Element:

$$dT = B\rho(\Omega r - v_v - v_i)\Gamma dr - B(C_d/C_l)(u + U_\infty)\rho\Gamma dr \quad (11)$$

$$dQ = B\rho(u + U_\infty)\Gamma rdr + B(C_d/C_l)(\Omega r - v_v - v_i)\rho\Gamma rdr \quad (12)$$

These four relations for thrust and torque (Eqs. 9 - 12) yield two equations for two unknowns ( $u$ ,  $v_i$ ) for each differential blade element. The other three unknown quantities ( $\Gamma$ ,  $\kappa$ , and  $v_v$ ) are treated as dependent functions of the input parameters: the lift distribution, rotor speed, ascent rate, number of blades, and chord distribution.

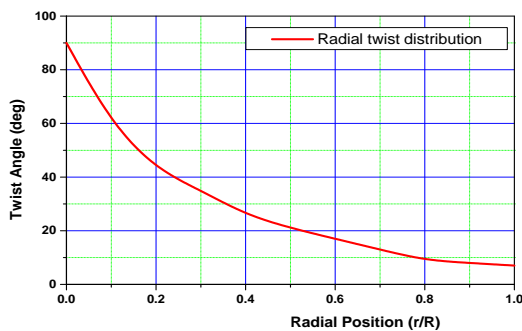
With values for  $u$  and  $v_i$ , the required blade pitch distribution,  $\theta(r)$  may be found as:

$$\theta(r) = \alpha_{geo} + \text{atan}\left(\frac{U_\infty + u}{\Omega r - v_i - v_v}\right) \quad (13)$$

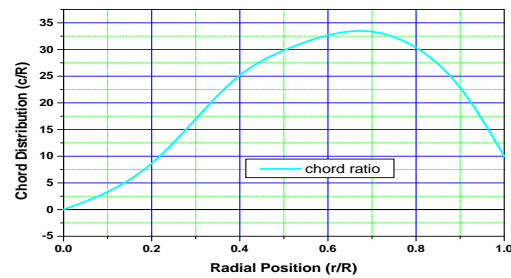
The determination of angle  $\theta(r)$  distribution is the last step in what can be described as the design case (Table 2, Fig. 7 a,b ).

Table 2 – Initial geometry of propeller

r/R	0.2	0.3	0.4	0.5	0.6	0.7	0.8	0.9	1.0		
Chord [mm]	8	17	26	30	33	34	31	24	10	D Diameter [mm]	380
$\theta$ [deg]	43	35	26	21	18	13	9	8	7	B Number of blades	3



a)



b)

FIG. 7. Radial twist (a) and chord (b) distribution of the blade

### 3. PERFORMANCE CHARACTERISTICS OF THE PROPELLER

#### 3.1 Analysis Tools

As mentioned before, for the first phase of the propeller design it is adequate to use computational methods based on the blade element momentum theory. Currently, there exist few available open sources, such as JBLADE [11], JAVAPROP [12], QPROP [13], or XROTOR [14] that can be used for this purpose. To analyze the aerodynamic characteristics of the given geometric configuration of the UAV propeller, in this study, the open source JBLADE is used.

JBLADE is an open-source propeller design and analysis code written in programming language. The code is based on David Marten’s QBLADE [15] and André Deperrois’ XFLR5 [16].

The airfoil performance figures needed for the blades simulation come from QBLADE’s coupling with the open-source code XFOIL [17]. This integration, which is also being improved, allows for the fast design of custom airfoils and computation of their polars.

JBLADE uses the classical Blade Element Momentum (BEM) theory modified to account for the 3D flow equilibrium, already presented in the previous sections.

The code can estimate the performance curves of a given propeller design for off-design analysis. The software has a graphical interface making it easier to build and analyze the propeller simulations. The code structure is presented in Figure 8.



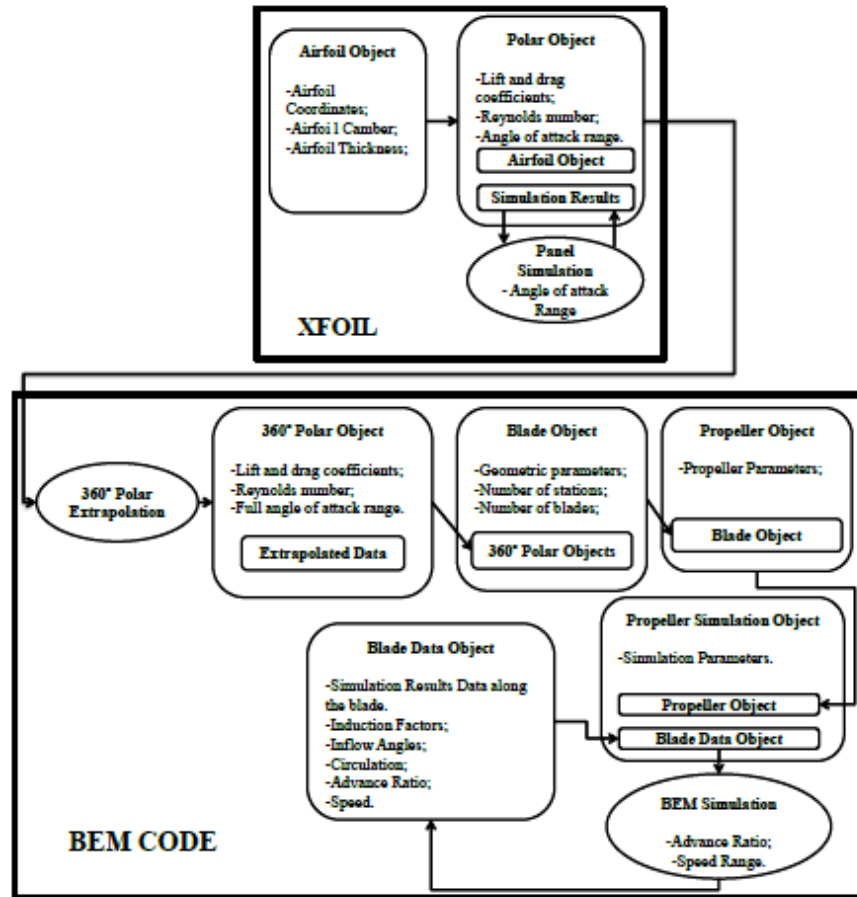


FIG. 8. JBLADE code structure [11]

Comparing with JAVAPROP and QPROP, JBLADE gives the best overall results.

### 3.2 Input Data

It has been considered that the investigated propeller propels a Hirus UAV, having the characteristics given in Fig. 9. It has been mentioned that when beginning to design a propeller one must know which is the motor that rotates it and what is the flight mission of the UAV.

Wingspan	2,35 m
Length	1,1 m
MTOW	7 kg
Maximum speed	130 km/h
Cruise speed	90 km/h
Radius of operation:	15 km
Ceiling height	3000 m
Propulsion	electric
Endurance	180 min
Launch system	<u>autorun</u>
Recovery system –	parachute
Maximum payload	0,9 kg


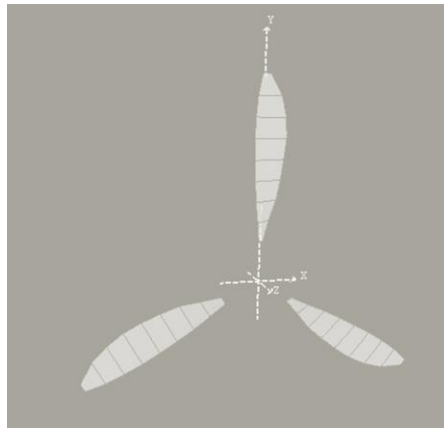


FIG. 9. Characteristics data of Hirus UAV

The blade geometry can be introduced as an arbitrary number of sections characterized by their radial position, chord, twist, length and airfoil coordinates. The propeller number of blades and hub radius must be specified as well.

The given geometry of the investigated propeller (Fig.10) consists of:

- Blade airfoil :                    Eppler 387 (it can be optimized in XFOIL )
- Blade radius:                     $R=0.190$  m
- Hub radius:                       $r_h=0.017$  m
- Number of blade:                 $B=3$
- Number of blade elements:  $n_e=20$
- Chord distribution,  $c(r)$  :    see Table 3
- Pitch distribution,  $\theta(r)$  :    see Table 3

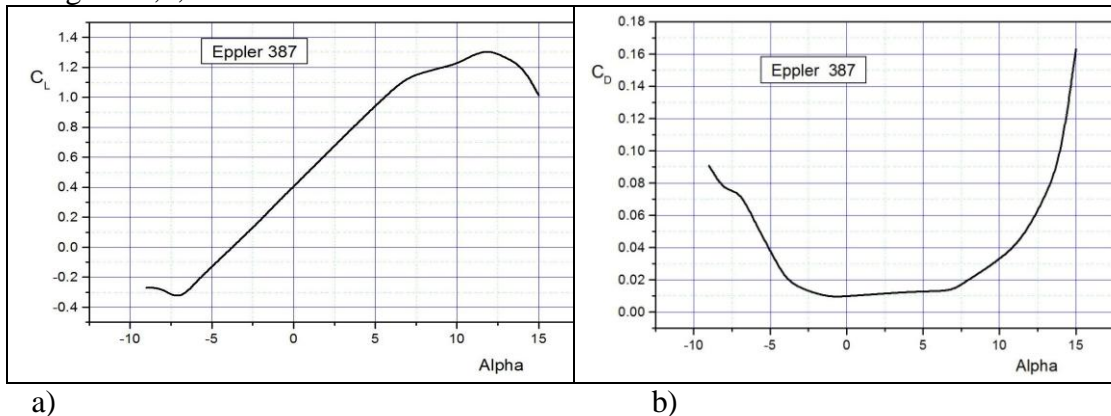


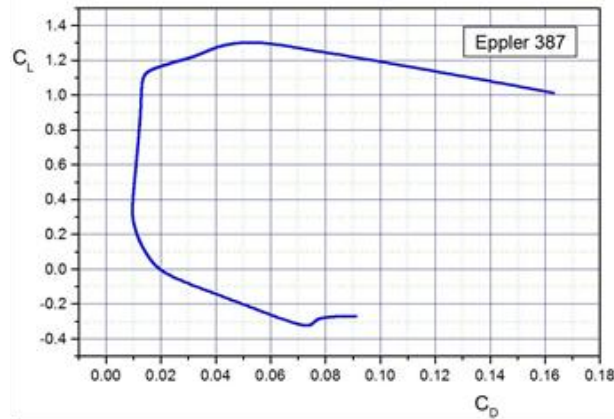
**FIG. 10.** The geometry of the 3-blade rotor

Additional input data:

- Altitude:                         $h = 200$  m
- Density:                         $\rho = 1.21$  kg/m<sup>3</sup>
- Cruise speed:                 $V = 25$  m/s
- Rotation speed:               $N = 5500$  r.p.m.  
 $\Omega = 576$  rad/s  
 $n = 92$  r.p.s.

The Eppler 387 polar data, obtained in Sub-Module XFOIL, are presented graphically in Fig. 11 a,b,c.





c)

FIG. 11. Eppler 387 Polar : a)  $C_L(\alpha)$ , b)  $C_D(\alpha)$  and c)  $C_L(C_D)$ , ( $Re=200000$ ).

#### 4. NUMERICAL RESULTS AND DISCUSSIONS

Given the advance ratio  $J$ , the geometric description of the propeller: the diameter  $D$ , the number of blades  $B$ , the pitch angle distribution  $\theta(\bar{r})$ , chord distribution  $c(\bar{r})$ , sectional aerodynamic characteristics, the lift ( $C_L$ ) and drag ( $C_D$ ) coefficients and another input data (section 3.2), using open source JBLADE, based on BEMT, off-design performance characteristics curves of this propeller have been obtained: power coefficient (Fig. 12), thrust coefficient (Fig. 13), propeller efficiency versus advance ratio (Fig. 14), as well as values for thrust, power or torque (Fig. 15).

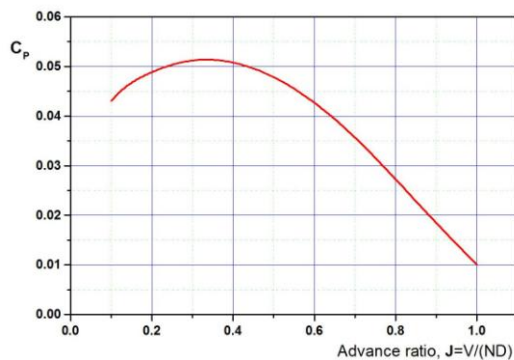


FIG. 12. Power coefficient versus advance ratio

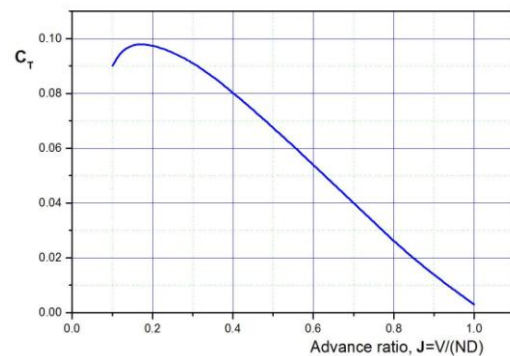


FIG. 13. Thrust coefficient versus advance ratio

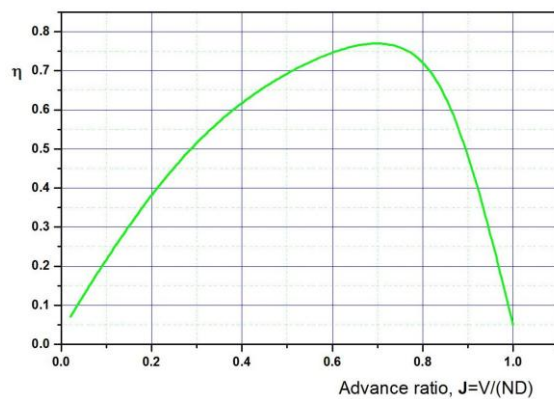


FIG. 14. Propeller efficiency versus advance ratio

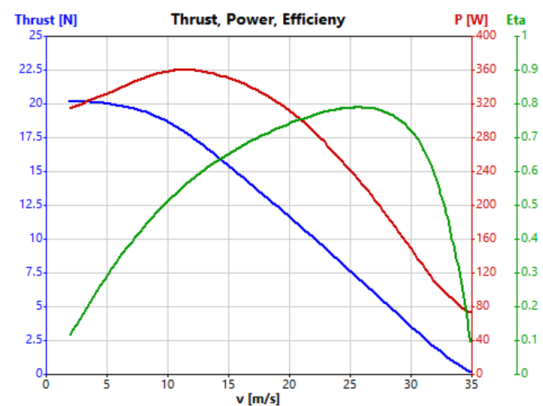


FIG. 15. Thrust, power and propeller efficiency versus cruise speed

There is no experimental data for this configuration of the propeller, but in previous calibration investigations and comparisons of different methods of computing it was noticed that JBLADE predicts closely the thrust coefficient. However, the power coefficient is under predicted at low advance ratios and slightly overestimated at higher final advance ratio values.

A first reason for these differences can be attributed to the airfoil's  $360^{\circ}$  angle of attack range airfoil polar obtained by extrapolation in XFOIL (3D rotational effect in the root portion of the blade is not enough quantified) and, furthermore, the constant axial induced velocity across the propeller disk is not seen to be the best assumption.

However, these results can be considered useful for a first design stage and can be considered as initial data in a subsequent optimization process. This is possible because it can be analyzed several configurations and regimes operating in a short time and at a reduced cost.

## 5. CONCLUSIONS

A method of preliminary design and analysis of propellers for small UAVs has been proposed, based on BEM theory. The design procedure has created the blade geometry in terms of the chord distribution along the radius as well as the distribution of the blade angle.

A case study on the profiles used for low Reynolds numbers has been carried out.

The used analysis method, less expensive, can be successfully used in a program to optimize the initial solution.

In the follow-up, other methods can be used to calculate more accurate solutions (CFDs) and experimental tests for the wind tunnel and even the flight tests will be required to ensure that the solution is optimal and the product may be passed into manufacturing.

## REFERENCES

- [1] H. Dumitrescu, A. Georgescu, A. Dumitrache, V. Ceanga, J.S. Popovici, Gh. Ghita, B. Nicolescu, *Calculus of propellers, / (Calculul elicei)*, Romanian Academy Publishing House, Bucharest, 1990;
- [2] H. Dumitrache, V. Cardos, A. Dumitrache, *Aerodynamics for wind turbines / (Aerodinamica turbinelor de vânt)*, Romanian Academy Publishing House, Bucharest, 2001;
- [3] A. Altman, *A Conceptual Design Methodology for Low Speed High Altitude Long Endurance Unmanned Aerial Vehicles*, Thesis, Cranfield University, 2000;
- [4] Glauert, H., "Airplane propellers," *Aerodynamic theory*, Durand WF, ed., Berlin: 1935;
- [5] I.P. Tracy, *Propeller Design and Analysis for a Small, Autonomous UAV, Methodology for Low Speed High Altitude Long Endurance Unmanned Aerial Vehicles*, Thesis, Massachusetts Institute of Technology, 2011;
- [6] M.F. Shariff, *Propeller Aerodynamic Analysis and Design*, AERO2365 Thesis, RMIT University, 2007
- [7] W. M. J., Rankine, and R. E., Froude, *On the Mechanical Principles of the Action of the Propellers*, Trans Inst Naval Architects (British), 1889;
- [8] Ma, R., Zhong, B. & Liu, Optimization design study of low-Reynolds-number high-lift airfoils for the high-efficiency propeller of low-dynamic vehicles in stratosphere, P. Sci. China Technol. Sci., 53: 2792, 2010;
- [9] J. Corrigan, and J. Schillings, Empirical Model for Blade Stall Delay Due to Rotation, *American Helicopter Society Aeromechanics Specialists*, San Francisco: 1994;
- [10] J. L. Tangier, M. S. Selig, An evaluation of an empirical model for stall delay due to rotation for HAWTs. NREL/CP-440-23258, 1997;
- [11] Silvestre, M. A. R., Morgado, J. and Páscoa, J. C., JBLADE: a Propeller Design and Analysis Code, AIAA 2013-4220, 2013 International Powered Lift Conference, August 12-14, Los Angeles, CA., 2013;
- [12] M. Hepperle, JAVAPROP-User Guide , Last Revision January 2015;
- [13] M. Drela, *QPROP Formulation*, 2006;
- [14] M. Drela, XROTOR Propeller and Windmill Design/Analysis software. [Online]. Massachusetts Institute of Technology Home Page. Available: <http://web.mit.edu/drela/Public/web/xrotor> ;
- [15] D. Marten, and J. Wendler, *QBlade Guidelines v0.6*, Berlin: 2013;
- [16] A. Deperrois, *Analysis of Foils and Wings Operating at Low Reynolds Numbers - Guidelines for XFLR5 v6.03*, 2011;
- [17] Drela, M., XFOIL - An Analysis and Design System for Low Reynolds Number Airfoils, *Low Reynolds Number Aerodynamics*, T.J. Mueller, ed., Berlin: Springer-Velag, pp. 1–12, 1989;
- [18] \*\*\* Ansys Fluent Theory Guide.